

NJC

Accepted Manuscript



This is an *Accepted Manuscript*, which has been through the Royal Society of Chemistry peer review process and has been accepted for publication.

Accepted Manuscripts are published online shortly after acceptance, before technical editing, formatting and proof reading. Using this free service, authors can make their results available to the community, in citable form, before we publish the edited article. We will replace this *Accepted Manuscript* with the edited and formatted *Advance Article* as soon as it is available.

You can find more information about *Accepted Manuscripts* in the [Information for Authors](#).

Please note that technical editing may introduce minor changes to the text and/or graphics, which may alter content. The journal's standard [Terms & Conditions](#) and the [Ethical guidelines](#) still apply. In no event shall the Royal Society of Chemistry be held responsible for any errors or omissions in this *Accepted Manuscript* or any consequences arising from the use of any information it contains.

Attracting interest for the past several decades, the field of catalytic oxidation is continuously and rapidly growing. Catalytic oxidation of benzylic C-H bond is one of the key transformations in organic synthesis and has a broad application in the manufacture of agrochemicals and pharmaceuticals.^{9,10} In spite of the high conversion, benzylic C-H bond oxidation reactions reported to date largely rely on homogeneous catalysis and hence recyclability of these often very expensive catalysts can be problematic.¹¹ Recently, the use of environment friendly oxidants, such as oxygen, hydrogen peroxide or *tert*-butyl hydroperoxide (TBHP) combined with noble transition metal heterogeneous catalysts was of particular interest for replacing their homogenous counterparts.¹²⁻¹⁴ Hence, the development of a benzylic C-H bond oxidation reaction with a novel and inexpensive heterogeneous catalyst of low toxicity would be of considerable interest and importance.

Amines are important building blocks of functional materials, additives, dyes, agrochemicals and pharmaceuticals.¹⁵ Since controlled mono alkylation of primary amines remains a challenge,^{16,17} synthesis of secondary amines rely much on the reductive amination reactions.¹⁸ Domino reductive amination, using nitroarenes is attractive as it does not require prior reduction of the nitroarenes.¹⁹⁻²⁴ The traditional methods for reductive aminations involve the use of stoichiometric chemical reagents, such as LiAlH_4 , NaBH_4 or the use of corrosive acetic acid which poses various limitations both economically and environmentally.²⁵ Thus, methods involving the use of molecular hydrogen and recyclable catalysts are often the most preferred pathways to reduce an organic compound.

In this paper, we reported a facile and novel methodology for the synthesis of palladium nanoparticles onto amine functionalized inorganic/organic magnetic composite $[\text{Fe}_3\text{O}_4@\text{SiO}_2/\text{EDAC-Pd}(0)]$ which represent an excellent example of synergism of the properties of both inorganic and organic components. The catalytic activity of the novel $\text{Fe}_3\text{O}_4@\text{SiO}_2/\text{EDAC-Pd}(0)$ was tested in the oxidation of benzylic C-H bond using TBHP and for the one-pot reductive

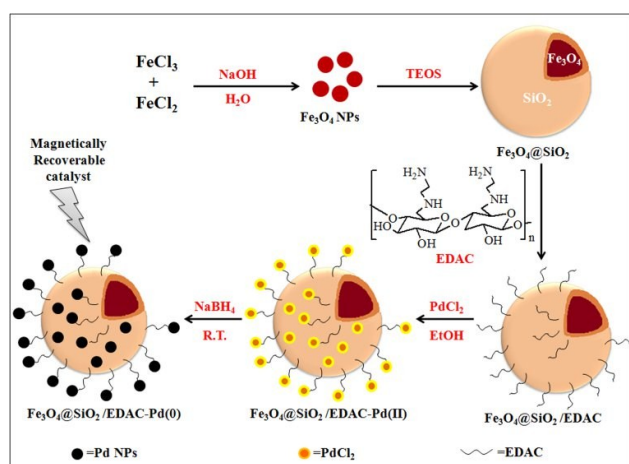
amination of aldehydes with nitroarenes using molecular hydrogen. Further, the catalyst proved its excellent potential in both reactions and could be reused efficiently with upto 6 consecutive runs with high efficiency.

Results and Discussion

Characterization of palladium nanoparticles onto amine functionalized inorganic/organic magnetic composite $[\text{Fe}_3\text{O}_4@\text{SiO}_2/\text{EDAC-Pd}(0)]$

The general procedure for the synthesis of $\text{Fe}_3\text{O}_4@\text{SiO}_2/\text{EDAC-Pd}(0)$ is represented in **Scheme 1**. It involves the co-precipitation of Fe^{3+} and Fe^{2+} salts to get Fe_3O_4 nanoparticles, followed by the formation of silica spheres²⁶ onto the surface of the Fe_3O_4 nanoparticles by sol-gel process. Although, Fe_3O_4 embedded SiO_2 spheres are quite stable but the aggregation and leaching of metal nanoparticles from their surface remains the drawback. In this regard, binding of Fe_3O_4 embedded SiO_2 spheres i.e., $\text{Fe}_3\text{O}_4@\text{SiO}_2$ with natural biopolymers provides more stability. The chemical modification of cellulose was done by incorporating the ethylene-1,2-diamine moiety as a pendant chain covalently bonded to the main polymeric framework which gives further stability. The inorganic/organic hybrid magnetite nanoparticles were prepared via formation of covalent bonds between ethylene diamine functionalized cellulose (EDAC) and silica coated Fe_3O_4 . Further, EDAC also acts as a surfactant,²⁷ which restricts the agglomeration and/or growth of the nanoparticles. Palladium nanoparticles were then immobilized onto the surface of ethylene diamine functionalized inorganic/organic substrate by in situ reduction of palladium chloride using NaBH_4 . During this process, the distribution of the size of Pd nanoparticles onto the surface of $\text{Fe}_3\text{O}_4@\text{SiO}_2/\text{EDAC}$ was controlled by the slow addition of NaBH_4 over a time period of 6, 8 and 10 h. It has been observed that, when NaBH_4 was added during 6 h, the size of Pd (0) nanoparticles obtained was in the range of 10-15 nm (HRTEM image and particle size histogram, **Fig. S1**, see ESI). But, when we increased the time of NaBH_4 addition for 8 h, a comparatively smaller Pd(0) nanoparticles in the size

range of 6-10 nm were obtained (**Fig. 3**). While, further increase in the time of NaBH_4 addition to 10 h gave the similar results. The prepared novel magnetic catalyst, $\text{Fe}_3\text{O}_4@/\text{SiO}_2/\text{EDAC-Pd}(0)$ was characterized by different techniques such as fourier transform infrared (FT-IR) spectroscopy, thermogravimetric analysis (TGA), X-ray diffraction (XRD), scanning electron microscopy (SEM), high resolution transmission electron microscopy (HRTEM), energy dispersive X-ray (EDX) analysis, inductively coupled plasma atomic emission spectroscopy (ICP-AES), X-ray photoelectron spectroscopy (XPS) and vibrating sample magnetometry (VSM).



Scheme 1. General procedure for the synthesis of $\text{Fe}_3\text{O}_4@/\text{SiO}_2/\text{EDAC-Pd}(0)$.

The surface modification of the prepared materials was characterized by FTIR spectroscopy. FT-IR spectra of $\text{Fe}_3\text{O}_4@/\text{SiO}_2$ (a), $\text{Fe}_3\text{O}_4@/\text{SiO}_2/\text{EDAC}$ (b) and $\text{Fe}_3\text{O}_4@/\text{SiO}_2/\text{EDAC-Pd}(0)$ (c) is shown in **Fig. 1**. The characteristic peaks around 1111, 800 and 475 cm^{-1} were observed due to SiO_2 bonds, while the characteristic peak around 582 cm^{-1} was observed due to the presence of Fe-O bond (**Fig. 1a, b and c**). Further, the IR spectrum of $\text{Fe}_3\text{O}_4@/\text{SiO}_2/\text{EDAC-Pd}(0)$ (**Fig. 1b**) characterized by the broad peak centred around 3400 cm^{-1} was an envelope of stretching vibrations for O-H of the adsorbed water, silanol groups, and N-H of the ethylene diamine functionalized cellulose. Two additional bands around 2895 and 1615 cm^{-1} were observed due to the stretching vibrations of the C-H of CH_2 groups and the bending vibrations of the -NH of the NH_2

groups respectively, both of which were associated with ethylene diamine modified $\text{Fe}_3\text{O}_4@/\text{SiO}_2/\text{EDAC}$ (**Fig. 1b and 1c**). The FT-IR spectra provided evidence of the formation of a silica shell onto the surface of Fe_3O_4 and also indicated that the ethylene diamine functionalized cellulose was successfully grafted onto $\text{Fe}_3\text{O}_4@/\text{SiO}_2$.

The thermal stability of $\text{Fe}_3\text{O}_4@/\text{SiO}_2/\text{EDAC-Pd}(0)$ was examined by thermo gravimetric analysis (**Fig. 2**). The TGA was recorded by heating the sample at the rate of $10\text{ }^\circ\text{C min}^{-1}$.

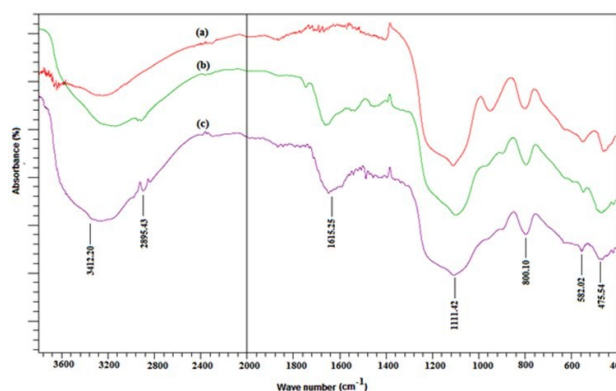


Fig. 1 FTIR spectra of $\text{Fe}_3\text{O}_4@/\text{SiO}_2$ (a), $\text{Fe}_3\text{O}_4@/\text{SiO}_2/\text{EDAC}$ (b) and $\text{Fe}_3\text{O}_4@/\text{SiO}_2/\text{EDAC-Pd}(0)$ (c).

The TGA curve of $\text{Fe}_3\text{O}_4@/\text{SiO}_2/\text{EDAC-Pd}(0)$ showed an initial weight loss up to $150\text{ }^\circ\text{C}$, which was attributed to the loss of residual solvent and water trapped onto the surface. The major weight loss beyond $210\text{ }^\circ\text{C}$ may be attributed to the decomposition of cellulose and chemisorbed material i.e. ethylene diamine groups present in the modified $\text{Fe}_3\text{O}_4@/\text{SiO}_2/\text{EDAC}$ substrate. Thus, the catalyst is reasonably stable up to $210\text{ }^\circ\text{C}$ and it is safe to carry out the reaction under heterogeneous conditions.

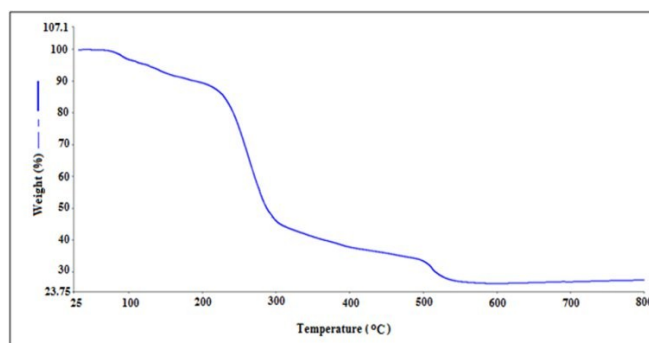


Fig. 2 TGA of $\text{Fe}_3\text{O}_4@/\text{SiO}_2/\text{EDAC-Pd}(0)$.

The formation of Pd(0) nanoparticles was confirmed through X-ray powder diffraction studies (**Fig. S2, see ESI**), which showed three reflection patterns at $2\theta = 39.9, 46.0,$ and 68.2° corresponding to the (111), (200) and (220) crystalline planes of face-centered cubic (fcc) Pd.²⁸ Further, the diffraction peaks at $2\theta = 30.1, 35.5, 57.1$ and 62.3° corresponds to the (111), (220), (311) and (511) planes of cubic phase of Fe_3O_4 lattice.²⁹ In addition, a broad diffraction peak at $2\theta = 20\text{--}25^\circ$ was assigned to amorphous silica coated on the surface of Fe_3O_4 nanospheres.

The surface morphology of $\text{Fe}_3\text{O}_4@/\text{SiO}_2/\text{EDAC-Pd}(0)$, was determined by SEM analysis (**Fig. 4a and 4b**). The SEM images showed that the catalyst was a homogeneous powder and Pd nanoparticles were uniformly distributed onto the surface of $\text{Fe}_3\text{O}_4@/\text{SiO}_2/\text{EDAC}$, and most of the particles have quasi-spherical shape. The HRTEM images provided a direct observation of the morphology and distribution of palladium nanoparticles onto the surface of $\text{Fe}_3\text{O}_4@/\text{SiO}_2/\text{EDAC}$ (**Fig. 3c and 3d**). The HRTEM image (**Fig. 3c**) of $\text{Fe}_3\text{O}_4@/\text{SiO}_2/\text{EDAC-Pd}(0)$ exhibited the presence of spherical particles which were observed in SEM micrographs also. Further, the inset image in **Fig. 3c**, reveals the formation of Fe_3O_4 core with a diameter of 240 nm and an outer shell thickness of Silica/EDAC was about 85 nm. **Fig. 3d** of the $\text{Fe}_3\text{O}_4@/\text{SiO}_2/\text{EDAC-Pd}(0)$ catalyst revealed that plenty of Pd nanoparticles with nearly spherical morphology and good dispersibility were distributed on the surface of the modified $\text{Fe}_3\text{O}_4@/\text{SiO}_2/\text{EDAC}$. Furthermore, the size distribution of palladium nanoparticles onto the surface of $\text{Fe}_3\text{O}_4@/\text{SiO}_2/\text{EDAC}$ was determined through the histogram which was proposed according to the data, obtained from the HRTEM (**Fig. 3e**). The average size of Pd(0) nanoparticles was 8.5 nm which showed a close agreement with the values calculated by XRD data. The elemental composition of $\text{Fe}_3\text{O}_4@/\text{SiO}_2/\text{EDAC-Pd}(0)$ was analyzed by energy dispersive X-ray (EDX) spectroscopy and the outcome was acceptable with expected elements: iron, silicon, oxygen, carbon and palladium (**Fig. 3f**). Moreover, the weight percentage of Pd in $\text{Fe}_3\text{O}_4@/\text{SiO}_2/\text{EDAC-Pd}(0)$ was determined by inductively

coupled plasma atomic emission spectroscopy (ICP-AES). The results indicated that Pd content loaded onto $\text{Fe}_3\text{O}_4@/\text{SiO}_2/\text{EDAC}$ was 3.0 wt%.

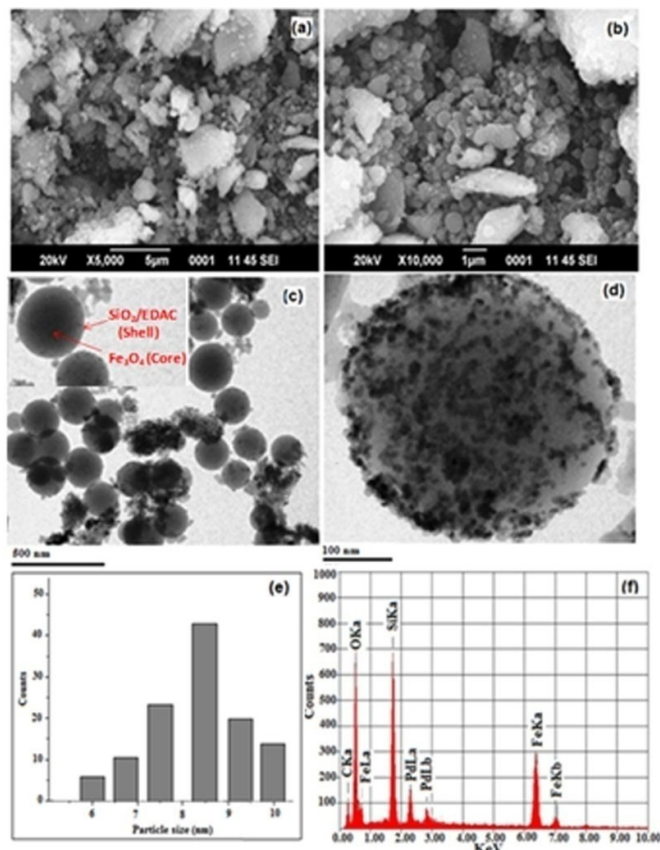


Fig. 3 SEM (a and b), HRTEM (c and d), particle size histogram (e) and EDX of $\text{Fe}_3\text{O}_4@/\text{SiO}_2/\text{EDAC-Pd}(0)$ (f).

X-ray photoelectron spectroscopy (XPS) technique was used to investigate the electron properties of the species formed on the surface of $\text{Fe}_3\text{O}_4@/\text{SiO}_2/\text{EDAC-Pd}(0)$, such as the oxidation state, and the binding energy of the core electron of the palladium metal. **Fig. 4a** shows the overall survey spectrum of $\text{Fe}_3\text{O}_4@/\text{SiO}_2/\text{EDAC-Pd}(0)$ in which peaks corresponding to carbon 1s (284.9 eV), oxygen 1s (532.2 eV), nitrogen 1s (401.4 eV), silica 2p (105.3 eV), iron 2p (712.1 eV) and palladium 3d (335.2 eV) are clearly observed. **Fig. 4b** shows the typical Pd(0) absorptions at 335.2 and 340.4 eV for $3d_{5/2}$ and $3d_{3/2}$ respectively, with a $\Delta = 5.2$ eV, which is consistent with the literature for Pd(0).³⁰

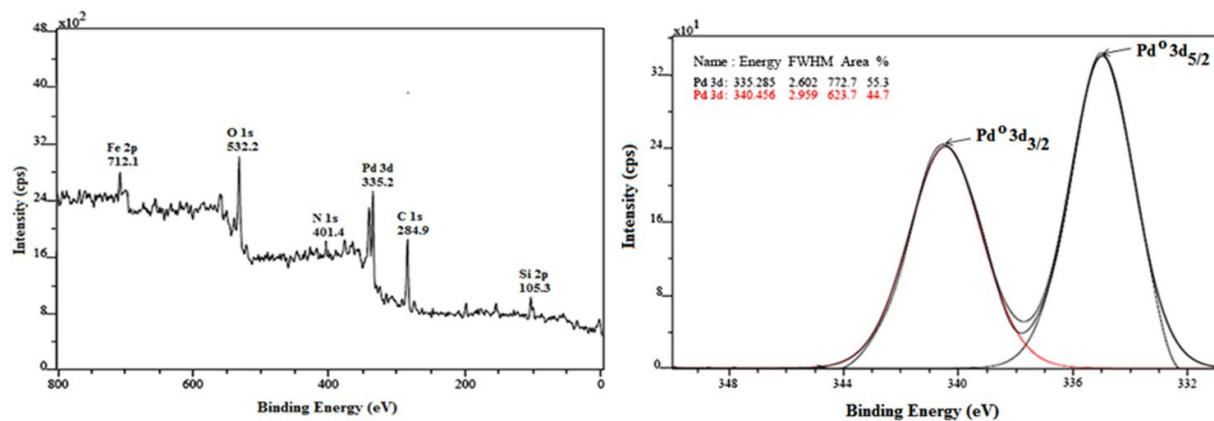


Fig. 4 XPS of $\text{Fe}_3\text{O}_4@/\text{SiO}_2/\text{EDAC-Pd}(0)$; overall survey spectrum (a) Pd 3d core level spectrum (b).

The magnetic properties of $\text{Fe}_3\text{O}_4@/\text{SiO}_2/\text{EDAC-Pd}(0)$ were evaluated by vibrating sample magnetometry (VSM) at room temperature (Fig. 5). The VSM magnetization curve illustrates magnetic saturation value of 38.7 emu/g with a characteristic hysteresis loop which exhibited a soft ferromagnetic behaviour. Fig. 5, also showed that the catalyst allow a facile separation from the reaction mixture using an external magnet.

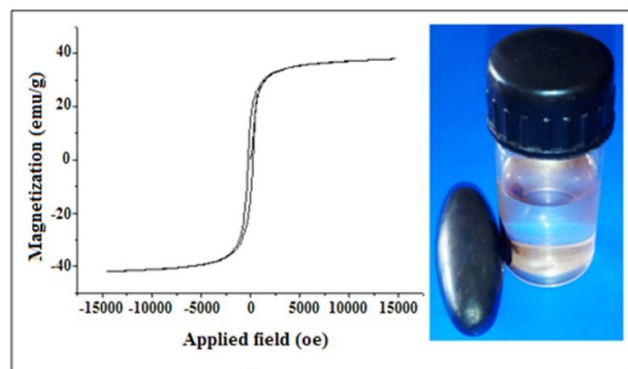
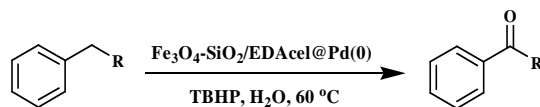


Fig. 5 Room temperature magnetization curve of $\text{Fe}_3\text{O}_4@/\text{SiO}_2/\text{EDAC-Pd}(0)$.

Catalyst testing for benzylic C-H bond oxidation

Initially, to obtain the most appropriate conditions for the desired protocol, the oxidation of ethylbenzene to

acetophenone was chosen as the model reaction (Scheme 2). Then, we set out to evaluate various experiments to compare the catalytic efficiency of $\text{Fe}_3\text{O}_4@/\text{SiO}_2/\text{EDAC-Pd}(0)$ with other catalysts and to optimize the appropriate catalytic amount required for the benzylic C-H bond oxidation. The results are summarized in Table 1. At first, the model reaction was performed in water without using any catalyst (Table 1, entry 1). No reaction was observed under this condition. Then, the model reaction was performed using 0.1 g of different catalyst systems, while keeping other conditions unaltered. Unfortunately, the yields obtained with other catalysts were not satisfactory (Table 1, entries 2-5). Further, we employed homogenous catalysts like PdCl_2 and $\text{Pd}(\text{OAc})_2$ to catalyse the benzylic C-H bond oxidation (Table 1, entries 6 and 7). With homogenous salts, the yields of the desired product were good but the reaction was not selective and many side products were formed. Further, we carried out the reaction using Pd(0) based heterogeneous systems (Table 1, entries 8 and 9) which resulted in satisfactory increase in yield of the desired product. Then, we examined the use of heterogeneous magnetic catalyst, $\text{Fe}_3\text{O}_4@/\text{SiO}_2/\text{EDAC-Pd}(0)$ for the model reaction. As can be seen from the results, the present catalyst, $\text{Fe}_3\text{O}_4@/\text{SiO}_2/\text{EDAC-Pd}(0)$ gave the desired product with



Scheme 2 $\text{Fe}_3\text{O}_4@\text{SiO}_2/\text{EDAC-Pd(0)}$ catalyzed C-H bond oxidation

Table 1. Optimization for the C-H bond oxidation and reductive amination

Entry	Catalyst	Amount (g)	C-H bond oxidation ^a		Reductive amination ^b	
			Time (h)	Yield (%) ^c	Time (h)	Yield (%) ^c
1.	-	-	10	traces	15	NR ^d
2.	SiO_2	0.1	10	traces	15	NR ^d
3.	Fe_3O_4	0.1	10	35	15	20
4.	$\text{Fe}_3\text{O}_4@\text{SiO}_2$	0.1	10	42	15	20
5.	$\text{Fe}_3\text{O}_4@\text{SiO}_2/\text{NH}_2\text{cel}$	0.1	10	45	15	25
6.	Pd(OAc)_2	0.1	4.0	60	7.0	65
7.	PdCl_2	0.1	4.0	65	6.0	70
8.	Cellulose-Pd(0)	0.1	3.5	72	4.5	80
9.	Silica/Cellulose-Pd(0)	0.1	2.45	79	3.0	85
10.	$\text{Fe}_3\text{O}_4@\text{SiO}_2/\text{EDAC-Pd(0)}$	0.1	2.0	90	2.5	93
11.	$\text{Fe}_3\text{O}_4@\text{SiO}_2/\text{EDAC-Pd(0)}$	0.05	2.0	90	2.5	93
12.	$\text{Fe}_3\text{O}_4@\text{SiO}_2/\text{EDAC-Pd(0)}$	0.025	3.0	81	3.5	82

^aReaction conditions: ethyl benzene (1 mmol), 70% *t*-BuOOH (1.5 mmol), water (5 mL) at 60 °C.

^bReaction conditions: benzaldehyde (1 mmol), nitrobenzene (1.2 mmol), ethanol:water (3:1, 5 mL) under H_2 atmosphere at room temperature.

^cIsolated Yield

^dNR: No reaction.

maximum yield and selectivity in 2h (**Table 1, entry 10**). Fascinated by these results, we carried out the test reaction using 0.05 g (1.5 mol% Pd) of $\text{Fe}_3\text{O}_4@\text{SiO}_2/\text{EDAC-Pd(0)}$, while keeping other conditions unaltered and the results indicated no change in the yield of product (**Table 1, entry 11**), although, further reduction in the amount of $\text{Fe}_3\text{O}_4@\text{SiO}_2/\text{EDAC-Pd(0)}$ led to the decrease in the yield of product (**Table 1, entry 12**). These results clearly indicated that the type of catalyst as well as its appropriate amount is essential for the oxidation to occur. Further, the high surface area to volume ratio of palladium nanoparticles together with their distribution on the magnetic support, played a

significant role for the excellent behaviour of $\text{Fe}_3\text{O}_4@\text{SiO}_2/\text{EDAC-Pd(0)}$ in catalyzing the desired reaction.

Further, in order to optimize the reaction conditions with respect to solvents, oxidants and temperatures, the model reaction was examined under different set of conditions to obtain the best possible combination and the results are presented in **Table 2**. Initially, the effect of various solvents such as CH_2Cl_2 , DMF, CH_3CN and H_2O at temperatures ranging from R.T. to 100 °C was tested in case of the model reaction. As could be seen in **Table 2**, the reaction in CH_2Cl_2 and DMF gave the poorest yields (**Table 2, entries 1-7**), while the yields have been much

improved in case of CH₃CN (**Table 2, entries 8-10**), but the best results were obtained in H₂O at 60 °C (**Table 2, entry 12**). However, when we carried out the model reaction in water at elevated temperatures of 80 and 100 °C, it has led to decrease of selectivity of the product formation. Thus, 60 °C was the appropriate temperature selected for carrying out the desired reaction in water. Next, the effect of various oxidants i.e., O₂, H₂O₂ and TBHP was examined. The results indicated that the oxidation with TBHP gave the best results in terms of time, yield and selectivity. (**Table 2, entry 12**). However, the oxidation using O₂ and H₂O₂ gave the poor yields.

Table 2. Optimization of different solvents, oxidants and reaction temperatures for benzylic C-H bond oxidation^a

Entry	Solvent	Oxidant	Temp (°C)	Time (h)	Yield (%) ^b
1.	CH ₂ Cl ₂	TBHP	RT	3	15
2.	CH ₂ Cl ₂	TBHP	40	3	45
3.	CH ₂ Cl ₂	O ₂	40	3	Traces
4.	CH ₂ Cl ₂	H ₂ O ₂	40	3	Traces
5.	DMF	TBHP	90	3	32
6.	DMF	O ₂	90	3	20
7.	DMF	H ₂ O ₂	90	3	25
8.	CH ₃ CN	TBHP	80	2.5	80
9.	CH ₃ CN	O ₂	80	3	35
10.	CH ₃ CN	H ₂ O ₂	80	3	40
11.	H ₂ O	TBHP	RT	3	25
12.	H₂O	TBHP	60	2	90
13.	H ₂ O	TBHP	100	2	83
14.	H ₂ O	O ₂	100	3	Traces
15.	H ₂ O	H ₂ O ₂	100	3	15

^aReaction conditions: ethyl benzene (1 mmol), oxidant (1.5 mmol), catalyst (0.05 g, 1.5 mol% Pd) and solvent (5 mL).

^bIsolated Yield.

A thorough literature survey shows that the selective synthesis of acetophenone from ethylbenzene is a challenge to heterogeneous catalysts because selectivity towards acetophenone is mainly hampered due to the formation of other oxygenates depending upon the type of catalyst used. As can be seen from the results (**Table 1, entry 12**) obtained

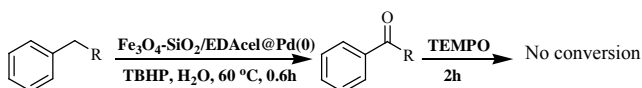
from the oxidation of ethyl benzene using Fe₃O₄@SiO₂/EDAC-Pd(0), the major product formed was acetophenone with high selectivity and other by-products were not observed. Thus, the mild reaction conditions, excellent stability and high yield for the transformation of ethylbenzene to acetophenone encouraged us to extend the scope of Fe₃O₄@SiO₂/EDAC-Pd(0) as heterogeneous catalyst to other benzylic hydrocarbons. As shown in **Table 3**, the oxidation of several benzylic C-H substrates to the corresponding products using Fe₃O₄@SiO₂/EDAC-Pd(0) proceeded smoothly with moderate to high yields. Ethyl benzene, fluorene, diphenylmethane and anthrone were efficiently converted to the corresponding ketone derivatives

(**Table 3, entries 1-4**). Cyclohexane was also converted to cyclohexanone under the same conditions (**Table 3, entry 5**).

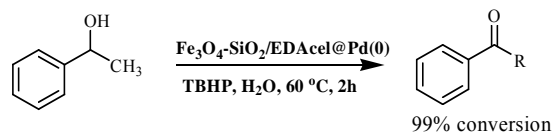
Extending the scope of the optimized conditions to other alkyl benzenes, it has been observed that toluene derivatives with electron-donating groups (**Table 3, entries 7-8**) undergo oxidation faster than those with electron-withdrawing counterparts (**Table 3, entries 9-10**). Moreover, when p-xylene was used, both methyl groups were oxidized to aldehydic groups, giving p-terephthaldehyde in good yield (**Table 3, entry 7**). The oxidation of toluenes to the corresponding benzoic acids, which is an important transformation in organic chemistry, could be efficiently achieved by increasing the reaction time. Thus, various toluene derivatives were tested and their corresponding acid derivatives were obtained in excellent yields (**Table 3, entries 11-13**). These results showed that Fe₃O₄@SiO₂/EDAC-Pd(0) can facilitate the oxidation of benzylic C-H bonds and serve as a highly efficient catalyst. A thorough literature survey showed no reference to the use of palladium nanoparticles onto inorganic/organic magnetic composite as catalysts for selective C-H bond oxidation.

To gather insights into benzylic C-H bond oxidation and to ascertain if the catalytic reaction involves a radical process, a radical-trapping experiment employing TEMPO (a radical scavenger) was performed (**Scheme 3a**). The first reaction (**Table 3, entry 1**) has been carried out until the conversion

was 45% (0.6 h) after which 1 mmole of TEMPO was added to it and the reaction was allowed to proceed further up to the completion (2 h). In this case, the reaction stopped, which could indicate that the oxidative transformation most likely occurred via radical intermediates. Based on the previous literature protocols, an alcohol derivative might be a possible intermediate in the formation of ketones. Thus, we also used 1-phenylethanol as the substrate under standard reaction conditions and almost quantitative yield was obtained (**Scheme 3b**), which indicates that the benzyl alcohol derivative may be an intermediate in the benzylic C-H bond oxidation.



Scheme 3a Radical trapping experiment



Scheme 3b Oxidation of 1-Phenylethanol

Catalyst testing for reductive amination of aldehydes with nitroarenes

Encouraged by the impressive performance of the $\text{Fe}_3\text{O}_4@\text{SiO}_2/\text{EDAC-Pd}(0)$ for C-H bond oxidation, we further explored the catalytic activity of the catalyst for the reductive amination reaction (**Scheme 4**). The reaction of benzaldehyde with nitrobenzene using molecular hydrogen at room temperature was chosen as a model reaction. Initial experiments were done for the comparison of its activity with other catalysts and for the optimization with respect to the amount of catalyst required for catalysing the desired reaction. The results are summarised in **Table 1**, which shows that 0.05 g (1.5 mol% Pd) of $\text{Fe}_3\text{O}_4@\text{SiO}_2/\text{EDAC-Pd}(0)$ showed best performance with respect to yield and time (**Table 1, entry 11**).

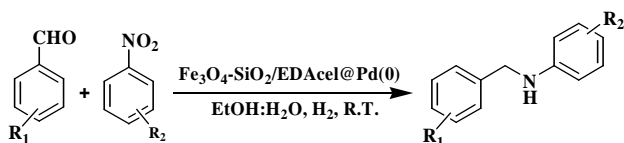
Table 3. C-H bond oxidation of arylalkanes catalyzed by $\text{Fe}_3\text{O}_4@\text{SiO}_2/\text{EDAC-Pd}(0)$ using TBHP under aqueous media at 60 °C^a

Entry	Substrate	Product	Time (h)	Yield (%) ^b
1.			2	90
2.			1.5	94
3.			1.5	95
4.			1.5	94
5.			1.5	88
6.			2	89
7.			3.25	88
8.			2.5	90
9.			3.75	90
10.			3.5	89
11.			4.5	88
12.			5.5	87
13.			4.5	86

^aReaction conditions: arylalkane (1 mmol), 70% *t*-BuOOH (1.5 mmol), $\text{Fe}_3\text{O}_4@\text{SiO}_2/\text{EDAC-Pd}(0)$ (0.05g, 1.5 mol% Pd) and water (5 mL) at 60 °C.

^bIsolated yield.

Next, we studied the effect of the solvent on reductive amination and observed that the nature of the solvent affected the conversion of the reaction. Solvents such as CH_2Cl_2 , EtOH, CH_3CN and H_2O were studied, but these solvents gave low yields for the reaction (**Table 4, entries 1-5**). However, when we chose organic/aqueous co-solvent system, high yields of 82% to 93% were obtained (**Table 4, entries 6-8**). This may be attributed to the beneficial effect of the co-solvent which resulted in good solubility of the organic substrates.



Scheme 4 Reductive amination of aldehydes with nitroarenes

Table 4. Effect of solvents for the reductive amination in the presence of $\text{Fe}_3\text{O}_4@\text{SiO}_2/\text{EDAC-Pd}(0)$ using molecular hydrogen at room temperature^a.

Entry	Solvent	Time (h)	Yield (%) ^b
1.	CH_2Cl_2	6	45
2.	H_2O	6	60
3.	CH_3CN	5	68
4.	MeOH	4.5	72
5.	EtOH	3	80
6.	EtOH/ H_2O (1:3)	3	82
7.	EtOH/ H_2O (1:1)	3	85
8.	EtOH/ H_2O (3:1)	2.5	93

^aReaction conditions: benzaldehyde (1 mmol), nitrobenzene (1.2 mmol), $\text{Fe}_3\text{O}_4@\text{SiO}_2/\text{EDAC-Pd}(0)$ (0.05g, 1.5 mol% Pd), solvent (5 mL) under H_2 atmosphere at room temperature.

^bIsolated yield.

With a reliable set of conditions in hand, the scope and generality of the developed protocol with respect to various aldehydes and nitroarenes were investigated using $\text{Fe}_3\text{O}_4@\text{SiO}_2/\text{EDAC-Pd}(0)$. As shown in **Table 5**, various aldehydes were reductively aminated with nitroarenes in EtOH/ H_2O (3:1) at room temperature under hydrogen atmosphere. Furthermore, reaction of most of the substrates with aromatic aldehydes and nitroarenes bearing electron-

donating as well as electron-withdrawing groups ran well and the corresponding products were obtained in good yields.

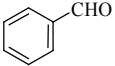
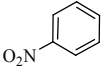
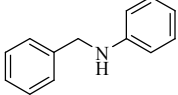
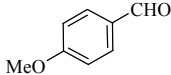
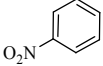
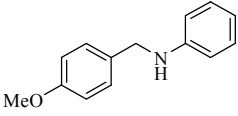
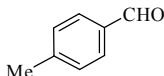
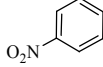
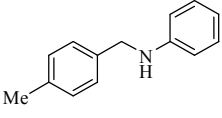
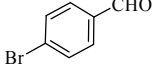
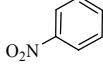
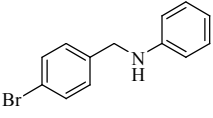
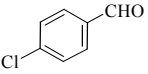
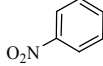
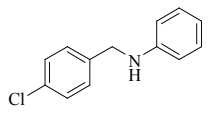
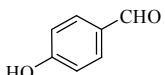
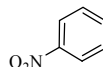
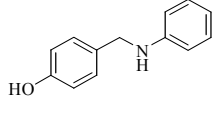
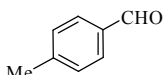
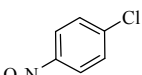
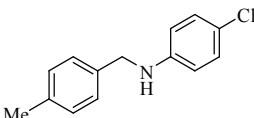
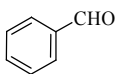
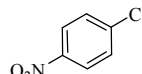
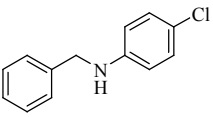
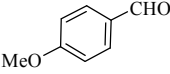
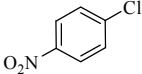
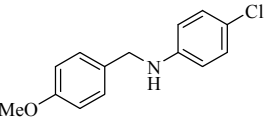
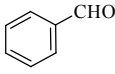
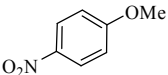
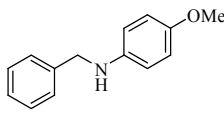
Comparison with other catalyst systems

In order to evaluate the uniqueness and efficiency of $\text{Fe}_3\text{O}_4@\text{SiO}_2/\text{EDAC-Pd}(0)$ catalyst among the different catalysts reported in literature, we have compiled the data for benzylic C-H bond oxidation and for the reductive amination, the results are collected in **Table 6 and 7**. The results show the supremacy of the present catalytic system in terms of time, yield and selectivity compared to others reported in the literature. Furthermore, the present protocol affords a truly green process using benign reaction media as well as achieving higher product yields in shorter reaction time.

Recyclability and heterogeneity

In sustainable organic synthesis, the recovery of the catalyst is of prime importance, which is generally accomplished via laborious filtration or centrifugation techniques. Due to the magnetic character of $\text{Fe}_3\text{O}_4@\text{SiO}_2/\text{EDAC-Pd}(0)$, the catalyst could be recovered easily using an external magnet. To confirm the reusability and stability of the catalyst, we carried out a set of experiments in case of **Table 3, entry 1** and **Table 5, entry 1** using $\text{Fe}_3\text{O}_4@\text{SiO}_2/\text{EDAC-Pd}(0)$. After completion of reaction, the catalyst was recovered using an external magnet, washed successively with EtOAc, double distilled water, and then dried. A fresh reaction was then setup using recovered $\text{Fe}_3\text{O}_4@\text{SiO}_2/\text{EDAC-Pd}(0)$ and new substrates were added under similar reaction conditions. $\text{Fe}_3\text{O}_4@\text{SiO}_2/\text{EDAC-Pd}(0)$ could be used at least six times without any change in activity. The results are summarized in **Table 8**. Further, to rule out the contribution of homogeneous catalysis, a reaction (**Table 3, entry 1**) was carried out until the conversion was 40% (0.5 h) and at that point the solid was filtered off at the reaction temperature. The liquid phase was then transferred to another flask and again allowed to react, but no further significant

Table 5. Reductive amination of aldehydes with nitroarenes catalyzed by $\text{Fe}_3\text{O}_4@\text{SiO}_2/\text{EDAC}-\text{Pd}(0)$ under molecular H_2 at room temperature^a

Entry	Aldehyde	Nitroarene	Product	Time (h)	Yield (%) ^b
1				2.5	93
2				3	91
3				2.5	90
4				3	89
5				2	91
6				3.5	90
7				3	88
8				2.5	90
9				3	90
10				3	89

^aReaction conditions: benzaldehyde (1 mmol), nitrobenzene (1.2 mmol), $\text{Fe}_3\text{O}_4@\text{SiO}_2/\text{EDAC}-\text{Pd}(0)$ (0.05g, 1.5 mol% Pd), ethanol:water (3:1, 5 mL) under H_2 atmosphere at room temperature.

^bIsolated yield.

Table 6 Comparison of the catalytic activity of $\text{Fe}_3\text{O}_4@\text{SiO}_2/\text{EDAC Pd}(0)$ with some reported catalytic systems for the C-H bond oxidation of ethylbenzene to acetophenone

Catalyst	Reaction conditions	Time /yield (h) (%)	Reference
CuI, L1 (Homogenous)	SDS, T-Hydro, H_2O , r.t.	1/68	31
$\text{Sc}(\text{OTf})_3$ (Homogenous)	RFT, CH_3CN , air, blue light (440 nm)	2.5/71	32
SUT-6-Zn (Heterogeneous)	TBHP, $\text{CH}_3\text{CN}/\text{AcOH}$, 65 °C	24/75	14
Ag/ZnO (Heterogeneous)	solvent-free, H_2O_2 , 80 °C	7/90	13
Cu-MOF-SiF ₆ (Heterogeneous)	TBHP, CH_3CN , 60 °C	48/38	33
$\text{Fe}_3\text{O}_4@\text{SiO}_2/\text{EDAC-Pd}(0)$ (Heterogeneous)	TBHP, H_2O, 60 °C	2/90	Present work

Table 7 Comparison of the catalytic activity of $\text{Fe}_3\text{O}_4@\text{SiO}_2/\text{EDAC-Pd}(0)$ with some reported catalytic systems for the reductive amination of benzaldehyde with nitroarene

Catalyst	Reaction conditions	Time/yield (h) (%)	Reference
HMMS-salpr-Pd	Ethanol, H_2 , R.T.	6/93	19
Pd NPs	Ethanol, H_2 , R.T.	6/92	20
$\text{Pd}_1\text{Ag}_{1.70}$	Ethanol, H_2 , R.T.	4/93	21
GA-Pd Nanoparticles	Methanol, H_2 , R.T.	6/88	22
Pd/ Fe_3O_4	Ethanol, H_2 , R.T.	6/92	23
Pd/ $\text{Fe}_3\text{O}_4@\text{C}$	Water, 60 °C, H_2	8/92	24
$\text{Fe}_3\text{O}_4@\text{SiO}_2/\text{EDAC-Pd}(0)$	EtOH/H_2O, H_2, R.T.	2.5/93	Present work

conversion was observed. This strongly suggests that the catalyst is heterogeneous in nature. Furthermore, the ICP-AES analysis of the used $\text{Fe}_3\text{O}_4@\text{SiO}_2/\text{EDAC}-\text{Pd}(0)$ after the 6th run was performed to calculate the Pd concentration. The initial concentration (3.0 wt% of Pd) before the reaction was reduced to 2.93 wt % after the 6th run. The small amount of Pd leaching may be due to microscopic changes that occurred on the surface of the magnetic catalyst. FTIR and TGA studies showed that the spent catalyst had no observable structural change relative to the fresh catalyst. Further, to examine the stability of Fe_3O_4 nanoparticles and $\text{Fe}_3\text{O}_4@\text{SiO}_2/\text{EDAC}$ under acidic conditions, 20 mg of each substrate was dispersed in 10 ml of HCl solution with concentrations of 0.05, 0.1, 0.1, and 0.15 mol/L, respectively. After continuous contact with acid for 2, 4 and 6 h, the suspension was magnetically separated and the leached iron concentration in the supernatant was determined by ICP-AES (Table 9). These results indicated that the coating of Fe_3O_4 with SiO_2/EDAC prevented the leaching of Fe to a major extent. However, we have not used acidic conditions in the reactions under study.

Table 8. Recyclability of $\text{Fe}_3\text{O}_4@\text{SiO}_2/\text{EDAC}-\text{Pd}(0)$ for the C-H bond oxidation and reductive amination reactions^a

Catalytic runs	C-H bond oxidation	Reductive amination
	Yield (%) ^b	Yield (%) ^b
1.	90	93
2.	90	93
3.	89	92
4.	88	92
5.	88	91
6.	87	91

^aReaction conditions [C-H bond oxidation]: ethyl benzene (1 mmol), 70% *t*-BuOOH (1.5 mmol), catalyst (0.05g, 1.5 mol% Pd) and water (5 mL) at 60°C; [Reductive amination]: benzaldehyde (1 mmol), nitrobenzene (1.2 mmol), catalyst (0.05g, 1.5 mol% Pd), ethanol:water (3:1, 5 mL) under H_2 atmosphere at room temperature. ^bIsolated Yield.

Table 9. Leaching test of Fe_3O_4 and $\text{Fe}_3\text{O}_4@\text{SiO}_2/\text{EDAC}$ under acidic environment.

Entry	HCl Sol. Conc. (M)	Leached Fe content (%)					
		Fe_3O_4			$\text{Fe}_3\text{O}_4@\text{SiO}_2/\text{EDAC}$		
		2 h	4 h	6 h	2 h	4 h	6 h
1	0.05	0.14	0.35	1.99	0.06	0.15	0.48
2	0.1	0.46	1.15	3.02	0.28	0.61	1.05
3	0.15	2.01	3.90	4.96	0.56	1.02	1.83

Conclusion

In conclusion, we have developed $\text{Fe}_3\text{O}_4@\text{SiO}_2/\text{EDAC}-\text{Pd}(0)$ as a novel, magnetic, and highly active heterogeneous catalyst for the benzylic C-H bond oxidation and reductive amination. The catalyst can be easily recovered using an external magnet and can be reused upto six times without significant deterioration in activity. The salient features of the proposed methodology include generality, operational simplicity, easy recyclability, a cleaner reaction profile which lead to short reaction time and high yields, thus adding a credit towards the development of greener methodologies for organic synthesis. Further investigations on the use of $\text{Fe}_3\text{O}_4@\text{SiO}_2/\text{EDAC}-\text{Pd}(0)$ catalyst for other potential transformations are being carried out in our laboratory.

Experimental

General

All the chemicals and solvents used were purchased from Aldrich Chemical Company or Merck. The ¹H and ¹³C NMR data were recorded in CDCl_3 on Bruker Avance III (400 MHz and 100 MHz) and mass spectral data on Bruker Esquires 3000 (ESI). The FTIR spectra were recorded on Perkin-Elmer FTIR spectrophotometer. TGA was recorded on Linsesis STA PT-1000 make thermal analyzer. X-ray diffratogram (XRD) was recorded on a Bruker AXSDB X-ray diffractometer using $\text{Cu K}\alpha$ radiations. SEM images were recorded using JEOL Model JSM-6390LV Scanning Electron

Microscope, High Resolution Transmission Electron Micrographs (HRTEM) were recorded on JEOL, JEM-2100F. EDX analysis was carried out on JEOL Model JED-2300 and the amount of metal in catalyst was determined by ICP-AES analysis using ARCOS from M/s Spectro, Germany. XPS spectra of the catalyst were recorded on a KRATOS ESCA model AXIS 165 (Resolution). VSM was measured using a vibrating sample magnetometer of Model: 7410 series, Lakeshore at room temperature from $-10\ 000$ to $+15\ 000$ Oe.

Synthesis of magnetite nanoparticles (Fe_3O_4 NPs)

FeCl_3 (5.0 g) and FeCl_2 (2.0 g) were successively dissolved in distilled water (30 mL). The resulting solution was then added dropwise into aqueous NaOH solution (1 M, 200 mL) under vigorous stirring for 30 minutes. The precipitation and formation of nanoferrites took place by a conversion of the metal salts into hydroxides and that, in turn, immediately transformed into ferrites. After 15 min, the precipitated ferrites were separated with a magnet and washed to $\text{pH} < 7.5$ by distilled water which were then dried under vacuum at $60\ ^\circ\text{C}$ over night.

Synthesis of silica coated magnetic nanoparticles ($\text{Fe}_3\text{O}_4@SiO_2$)

Fe_3O_4 (2 g) was dispersed in water (30 mL) followed by the addition of ethanol (120 mL), ammonia (6 mL) and TEOS i.e. tetraethyl orthosilicate (6 mL). The mixture was then refluxed for 6 h under vigorous stirring. The resulting $\text{Fe}_3\text{O}_4@SiO_2$ colloid was separated with magnet and washed repeatedly with distilled water (3×10 mL) and ethanol (3×10 mL). Then, the final product, $\text{Fe}_3\text{O}_4@SiO_2$ was dried in vacuum at $60\ ^\circ\text{C}$ over night.

Synthesis of ethylene diamine functionalized cellulose (EDAC)

Cellulose (5 g) previously activated at $80\ ^\circ\text{C}$ for 12 h was suspended in *N,N*-dimethylformamide (100 mL), followed by the slow addition of thionyl chloride (16 mL) at $80\ ^\circ\text{C}$, under mechanical stirring. After the addition was complete, stirring

was continued for another 4 h. The cellulose chloride (CeCl) obtained was washed with several aliquots of dilute ammonium hydroxide solution ($0.5\ \text{mol/L}\ \text{NH}_4\text{OH}$) and the supernatant after each treatment was removed to bring the pH to neutral. To complete the washing, the suspension was exhaustively treated with distilled water (2×100 mL). The solid was then separated by filtration and dried in vacuum at room temperature.

A mixture of CeCl (3 g) and ethylene-1,2-diamine (16 mL) was stirred at $116\ ^\circ\text{C}$ for 3 h. The reaction mixture was filtered through a sintered glass crucible and the solid was dried in vacuum at room temperature to afford EDAC as yellow powder.

Synthesis of ethylene diamine functionalized $\text{Fe}_3\text{O}_4@SiO_2/EDAC$

To a solution of $\text{Fe}_3\text{O}_4@SiO_2$ (2 g) in CHCl_3 (17 mL), EDAC (2 g) and triethyl amine (0.4 mL) were added, and the reaction mixture was stirred at $60\ ^\circ\text{C}$ for 12 h. $\text{Fe}_3\text{O}_4@SiO_2/EDAC$ was separated with magnet and washed with chloroform (3×10 mL) followed by water (3×10 mL) and dried under vacuum at $60\ ^\circ\text{C}$ over night.

Synthesis of palladium nanoparticles onto ethylene diamine functionalized $\text{Fe}_3\text{O}_4@SiO_2/EDAC-Pd(0)$

To a dispersed solution of $\text{Fe}_3\text{O}_4@SiO_2/EDAC$ (2 g) in ethanol (6 mL), aqueous solution of PdCl_2 (0.17 g, 1.0 mmol, 3 mL) was added, and the reaction mixture was stirred at room temperature for 6 h. Then, aqueous solution of NaBH_4 (1.2 mmol, 5 mL) was added slowly during 8 h. Finally, $\text{Fe}_3\text{O}_4@SiO_2/EDAC-Pd(0)$ was separated with magnet and washed successively with water (3×10 mL) and ethanol (3×10 mL). Finally, it was dried under vacuum at room temperature to give the dark polymeric Pd(0) nanoparticles (**Scheme 1**).

General procedure for the benzylic C-H bond oxidation

To a mixture of arylalkane (1 mmol), $\text{Fe}_3\text{O}_4@\text{SiO}_2/\text{EDAC-Pd}(0)$ (0.05 g, 1.5 mol% Pd) and 70% *t*-BuOOH (0.2 mL, 2 mmol) in a round bottom flask (25 mL), water (5 mL) was added, and the reaction mixture was stirred at 60 °C for an appropriate time (**Scheme 2**). After completion of the reaction (monitored by TLC), the catalyst was separated using an external magnet and the reaction mixture was diluted with ethyl acetate and filtered. The organic layer was washed with water and dried over anhyd. Na_2SO_4 . Finally, the product was obtained after removal of the solvent under reduced pressure followed by passing through column of silica gel and elution with EtOAc-pet. ether. The recovered catalyst was washed with EtOAc (3×5 mL) followed by double distilled water (3×10 mL). It was dried and then reused for subsequent reaction.

General procedure for the reductive amination

To a mixture of aldehyde (1 mmol), nitroarene (1 mmol) and $\text{Fe}_3\text{O}_4@\text{SiO}_2/\text{EDAC-Pd}(0)$ (0.05 g, 1.5 mol% Pd) in a round bottom flask (25 mL), EtOH:H₂O (3:1, 5 mL) was added, and the reaction mixture was stirred under H₂ atmosphere at room temperature for the appropriate time (**Scheme 4**). After completion of the reaction (monitored by TLC), the catalyst was separated using an external magnet and the reaction mixture was diluted with ethyl acetate and filtered. The organic layer was washed with water, dried over anhyd. Na_2SO_4 and concentrated under reduced pressure. The product was obtained after passing through column of silica gel and elution with EtOAc-pet. ether. The recovered catalyst was washed with EtOAc (3×5 mL) followed by double distilled water (3×10 mL). It was dried and then reused for subsequent reactions.

The structures of all the products were confirmed by ¹H, ¹³C NMR, mass spectral data and comparison with authentic samples obtained commercially or prepared according to the literature methods.

Acknowledgements

We thank the Head, SAIF, IIT Bombay for HRTEM and ICP-AES studies; Head, SAIF, Punjab University Chandigarh for XRD; Head, SAIF, Kochi for SEM, and EDX studies, ICT, Hyderabad for XPS analysis; and Head, CIF, Guwahati for VSM analysis. Financial assistance from UGC, New Delhi (SRF to one of the authors, MB and major research project, F 41-281/2012 SR) is gratefully acknowledged.

References

- (a) R. A. Sheldon and H. V. Bekkum (Eds.), *Fine Chemicals through Heterogeneous Catalysis*, Wiley-VCH: Weinheim, Germany, 2001; (b) J. F. Jenck, F. Agterberg and M. J. Droescher, *Green Chem.*, 2004, **6**, 544-556.
- (a) A. T. Bell, *Science*, 2003, **299**, 1688-1691; (b) M. A. El-Sayed, *Acc. Chem. Res.*, 2001, **34**, 257-264; (c) H. Yang, L. Zhang, P. Wang, Q. Yang and C. Li, *Green Chem.*, 2009, **11**, 257-264.
- (a) J. K. Cho, R. Najman, T. W. Dean, O. Ichihara, C. Muller and M. Bradley, *J. Am. Chem. Soc.*, 2006, **128**, 6276-6277; (b) M. L. N. Rao and R. J. Dhanorkar, *RSC Adv.*, 2013, **3**, 6794-6798; (c) M. Aydemir, A. Baysal, G. Ozturk, B. Gumgum, *Appl. Organomet. Chem.*, 2009, **23**, 108-113.
- (a) J. M. Campelo, D. Luna, R. Luque, J. M. Marinas, and A. A. Romero, *ChemSusChem*, 2009, **2**, 18-45; (b) A. K. Nezhad and F. Panahi, *Green Chem.*, 2011, **13**, 2408-2415.
- H. Q. Wang, X. Wei, K. X. Wang and J. S. Chen, *Dalton Trans.*, 2012, **41**, 3204-3208; (b) H. F. Wang, H. Ariga, R. Dowler, M. Sterrer and H. J. Freund, *J. Catal.*, 2012, **286**, 1-5; (c) W. Ludwig, A. Savara, B. Brandt and S. Schauer mann, *Phys. Chem. Chem. Phys.*, 2011, **13**, 966-977.
- J. Safari and Z. Zarnegar, *C. R. Chim.*, 2013, **16**, 821-828; (b) Y. H. Deng, C. H. Deng, D. W. Qi, C. Liu, J. Liu, X. M. Zhang and D. Y. Zhao, *Adv. Mater.*, 2009, **21**, 1377-1382. (c) C. Small and J. H. Johnston, *J. Colloids Interf. Sci.*, 2009, **331**, 122-126.

7. (a) F. He and D. Zhao, *Environ. Sci. Technol.*, 2005, **39**, 3314-3320; (b) S. Fischer, K. Thummler, B. Volkert, K. Hettich, I. Schmidt and K. Fischer, *Macromol. Symp.*, 2008, **262**, 89-96; (c) T. Tashiro, and Y. J. Shimura, *Appl. Polym. Sci.*, 1982, **27**, 747-756.
8. F. Zhang, J. Jin, X. Zhong, S. Li, J. Niu, R. Li and J. Ma, *Green Chem.*, 2011, **13**, 1238-1243; (b) A. J. Amali and R. K. Rana, *Chem. Commun.*, 2008, **44**, 4165-4167; (c) H. Veisia, J. Gholamib, H. Uedac, P. Mohammadia and M. Noroozid, *J. Mol. Catal. A: Chem.*, 2015, **396**, 216-223.
9. (a) M. Hudlicky, *Oxidations in Organic Chemistry*, ACS Monograph No. 186, American Chemical Society, Washington DC, 1990; (b) F. Recupero and C. Punta, *Chem. Rev.* 2007, **107**, 3800-3842.
10. (a) B. H. Brodsky and J. Du Bois, *J. Am. Chem. Soc.*, 2005, **127**, 15391-15393; (b) S. M. Lee and P. L. Fuchs, *J. Am. Chem. Soc.*, 2002, **124**, 13978-13979; (c) J. Genovino, S. Lutz, D. Sames and B. B. Toure, *J. Am. Chem. Soc.*, 2013, **135**, 12346-12352.
11. I. Hemeon, N. W. Barnett, N. Gathergood, P. J. Scammells and R. D. Singer, *Aust. J. Chem.*, 2004, **57**, 125-128.
12. (a) R. Raja and J. M. Thomas, *Chem. Commun.*, 1998, 1841-1842.
13. M. H. -Sarvari, T. A. -Kachouei and F. Moeini, *RSC Adv.*, 2015, **5**, 9050-9056.
14. H. Chen, Y. Deng, Z. Yu, H. Zhao, Q. Yao, X. Zou, J. E. Backvall and J. Sun, *Chem. Mater.*, 2013, **25**, 5031-5036.
15. A. Seayad, M. Ahmed, H. Klein, R. Jackstell, T. Gross and M. Beller, *Science*, 2002, **297**, 1676-1678.
16. D. M. Roundhill, *Chem. Rev.*, 1992, **92**, 1-27.
17. (a) M. S. Driver and J. F. Hartwig, *J. Am. Chem. Soc.*, 1996, **118**, 7217-7218; (b) D. Guo, H. Huang, J. Xu, H. Jiang and H. Liu, *Org. Lett.*, 2008, **10**, 4513-4516.
18. (a) R. P. Tripathi, S. S. Verma, J. Pandey and V. K. Tiwari, *Curr. Org. Chem.*, 2008, **12**, 1093-1115; (b) T. C. Nugent and M. E. -Shazly, *Adv. Synth. Catal.*, 2010, **352**, 753-819.
19. H. Liu, P. Wang, H. Yang, J. Niu and J. Ma, *New J. Chem.*, 2015, **39**, 4343-4350.
20. M. Nasrollahzadeh, *New J. Chem.*, 2014, **38**, 5544-5550.
21. L. Li, Z. Niu, S. Cai, Y. Zhi, H. Li, H. Rong, L. Liu, L. Liu, W. He and Y. Li, *Chem. Commun.*, 2013, **49**, 6843-6845.
22. B. Sreedhar, P. S. Reddy and D. K. Devi, *J. Org. Chem.*, 2009, **74**, 8806-8809.
23. S. Wei, Z. Dong, Z. Ma, J. Sun, J. Ma, *Catal. Commun.*, 2013, **30**, 40-44.
24. X. Zhou, X. Li, L. Jiao, H. Huo, R. Li, *Catal Lett.*, 2015, **145**, 1591-1599.
25. M. J. Bhanushali, N. S. Nandurkar, M. D. Bhor, B. M. Bhanage, *Tetrahedron Lett.*, 2007, **48**, 1273-1276.
26. (a) J. Kim, J. E. Lee, J. Lee, J. H. Yu, B. C. Kim, K. An, Y. Hwang, C. H. Shin, J. G. Park, J. Kim and T. Hyeon, *J. Am. Chem. Soc.*, 2006, **128**, 688-689; (b) S. I. Stoeva, F. Huo, J. S. Lee, and C. A. Mirkin, *J. Am. Chem. Soc.*, 2005, **127**, 15362-15363.
27. X. Di, S. K. Kansal and W. Deng, *Sep. Purif. Technol.*, 2009, **68**, 61-64.
28. H. Firouzabadi, N. Iranpoor and M. Gholinejad, *Tetrahedron*, 2009, **65**, 7079-7084.
29. S. Liu, F. Lu, X. Jia, F. Cheng, L. P. Jianga and J. J. Zhu, *CrystEngComm.*, 2011, **13**, 2425-2429.
30. J. F. Moulder, W. F. Stickle, P. E. Sobol, K. D. Bomben, *Handbook of X-ray Photoelectron Spectroscopy*, Physical Electronics Inc, USA, 1995, 118-119.
31. W. J. Ang and Y. Lam, *Org. Biomol. Chem.*, 2015, **13**, 1048-1052.
32. B. Muhldorf and R. Wolf, *Chem. Commun.*, 2015, **51**, 8425-8428.
33. S. Wang, L. Li, J. Zhang, X. Yuan and C.-Y. Su, *J. Mater. Chem.*, 2011, **21**, 7098-7104.

Graphical Abstract

$\text{Fe}_3\text{O}_4@\text{SiO}_2/\text{EDAC-Pd(0)}$ as a novel and efficient inorganic/organic magnetic composite: Sustainable catalyst for the benzylic C-H bond oxidation and reductive amination under mild conditions

Madhvi Bhardwaj^a, Harsha Sharma^a, Satya Paul^{a*} and James H. Clark^b

^aDepartment of Chemistry, University of Jammu, Jammu 180006, India. Fax: +91-191-2431365; Tel: +91-191-2453969; Email: pual7@rediffmail.com.

^bGreen Chemistry Centre of Excellence, Department of Chemistry, University of York, York, UK. Fax: +44 (0)1904 432705; Tel: +44 (0)1904 432567; E-mail: james.clark@york.ac.uk.

Magnetically recyclable ethylene diamine functionalized inorganic/organic composite, $\text{Fe}_3\text{O}_4@\text{SiO}_2/\text{EDAC-Pd(0)}$ for selective C-H bond oxidation and reductive amination under sustainable reaction media.

